AMERICAN SOCIETY FOR MICROBIOLOGY | Applied and Environmental Microbiology®

ENVIRONMENTAL MICROBIOLOGY

Carbaryl as a Carbon and Nitrogen Source: an Inducible Methylamine Metabolic Pathway at the Biochemical and Molecular Levels in *Pseudomonas* sp. Strain C5pp

Kamini,[a] Rakesh Sharma,[b] Narayan S. Punekar,[a] Prashant S. Phale[a]

[a]Department of Biosciences and Bioengineering, Indian Institute of Technology-Bombay, Mumbai, India
[b]Microbial Biotechnology and Genomics Unit, CSIR-Institute of Genomics and Integrative Biology, New Delhi, India

ABSTRACT Carbaryl is the most widely used carbamate family pesticide, and its persistent nature causes it to pollute both soil and water ecosystems. Microbes maintain the Earth's biogeochemical cycles by metabolizing various compounds present in the matter, including xenobiotics, as a sole source of carbon, nitrogen, and energy. Soil isolate *Pseudomonas* sp. strain C5pp metabolizes carbaryl efficiently as the carbon source. Periplasmic carbaryl hydrolase catalyzes the conversion of carbaryl to 1-naphthol and methylamine. 1-Naphthol was further used as a carbon source via gentisate, whereas the metabolic fate of methylamine is not known. Here, we demonstrate that strain C5pp showed efficient growth on carbaryl when supplied as a carbon and nitrogen source, suggesting that the methylamine generated was used as the nitrogen source. Genes involved in the methylamine metabolism were annotated and characterized at the biochemical and molecular level. Transcriptional and enzyme activity studies corroborate that the γ-glutamylmethylamide/*N*-methylglutamate (GMA/NMG) pathway is involved in the metabolism of carbaryl and methylamine as a nitrogen source. Compared to carbaryl, methylamine was found to be an effective inducer for the metabolic and transporter genes. Strain C5pp also harbored genes involved in sarcosine metabolism that were cotranscribed and induced by sarcosine. The presence of inducible pathways for metabolism of carbaryl as a nitrogen and carbon source helps in complete and efficient mineralization of carbaryl by strain C5pp, thereby maintaining the biogeochemical cycles.

IMPORTANCE The degradation of xenobiotics plays a significant role in the environment to maintain ecological systems as well as to prevent the imbalance of biogeochemical cycles via carbon-nitrogen cycling. Carbaryl is the most widely used pesticide from the carbamate family. *Pseudomonas* sp. strain C5pp, capable of utilizing carbaryl as a carbon and nitrogen source for its growth, subsequently helps in complete remediation of carbaryl. Thus, it maintains the ecosystem by balancing the biogeochemical cycles. The metabolic versatility and genetic diversity of strain C5pp for the transformation of contaminants like carbaryl and 1-naphthol into less harmful products make it a suitable candidate from the perspective of bioremediation.

KEYWORDS biogeochemical cycle, *Pseudomonas*, carbaryl, methylamine, nitrogen cycle, xenobiotics

The microbial oxidation of methylated amines is an important metabolic activity in biogeochemical cycling of carbon and nitrogen. This is an essential step in preventing the formation of methane, which is the second most important greenhouse gas, following carbon dioxide (1). Degradation of many nitrogenous compounds releases methylamine, e.g., putrefaction of proteins or degradation of pesticides (carbaryl, carbofuran, etc.) (2), and these methylamines do not accumulate in the environment, as

Received 1 August 2018 **Accepted** 1 October 2018

Accepted manuscript posted online 12 October 2018

Citation Kamini, Sharma R, Punekar NS, Phale PS. 2018. Carbaryl as a carbon and nitrogen source: an inducible methylamine metabolic pathway at the biochemical and molecular levels in *Pseudomonas* sp. strain C5pp. Appl Environ Microbiol 84:e01866-18. https://doi.org/10.1128/AEM.01866-18.

Editor Rebecca E. Parales, University of California, Davis

Address correspondence to Narayan S. Punekar, nsp@iitb.ac.in, or Prashant S. Phale, pphale@iitb.ac.in.

they are rapidly consumed by methylotrophs to produce biomass and CO_2 (3, 4). Methylamine also serves as the nitrogen source for several nonmethylotrophic microbes (5, 6). However, methylotrophs like *Methylobacterium extorquens* AM1 and *Paracoccus denitrificans* oxidize methylamine directly to formaldehyde and ammonia, a step that is catalyzed by a periplasmic methylamine dehydrogenase (MADH) (7, 8) or by methylamine oxidase (MAO) in Gram-positive methylotrophic bacteria such as *Arthrobacter* sp. strain P1 (9). Alternatively, in *Methylocella silvestris* and *Methylobacterium extorquens* DM4, methylamine is metabolized via methylated amino acid intermediates like γ-glutamylmethylamide (GMA) and *N*-methylglutamate (NMG) by employing γ-glutamylmethylamide synthase (GMAS) and *N*-methylglutamate synthase (NMGS), respectively. NMG is further oxidized to formaldehyde and glutamate by *N*-methylglutamate dehydrogenase (NMGDH) (2, 10). Formaldehyde, the end product of all methylamine oxidation pathways, is either oxidized to CO_2 or assimilated as a carbon source via the serine cycle or ribulose monophosphate pathway (11).

Carbaryl (1-naphthyl *N*-methylcarbamate) is the most widely used carbamate family insecticide. It acts by inhibiting the activity of acetylcholine esterase competitively, leading to muscle spasm, paralysis in insects, and finally death (12, 13). Carbaryl also affects other beneficial and nontargeted organisms, like earthworms and bees, and is classified as a potential human carcinogen (14, 15). *Rhodococcus, Arthrobacter, Micrococcus, Burkholderia,* and *Pseudomonas* spp. have been reported to degrade carbaryl as a sole source of carbon and energy (16–21). However, the metabolic fate of carbaryl as a nitrogen source has not been studied in these organisms.

Earlier, we reported a soil isolate, *Pseudomonas* sp. strain C5pp (here referred to as strain C5pp), that utilizes carbaryl as a source of carbon and energy (19). The degradation pathway is initiated in the periplasm by the hydrolysis of carbaryl into 1-naphthol, methylamine, and CO_2 by a carbaryl hydrolase (CH) (22). 1-Naphthol is further metabolized via the gentisate pathway (19). The fate of methylamine released from carbaryl is not known. The genome analysis revealed the presence of genes involved in nitrite and nitrate ammonification, ammonia assimilation, and methylamine metabolism (15). The objective of this study was to determine the role of methylamine as a nitrogen source for strain C5pp. We elucidated the degradation pathway of carbaryl when strain C5pp was provided with carbaryl as the nitrogen source. In the absence of any other external nitrogen source, strain C5pp showed growth on carbaryl, suggesting that it has the ability to utilize it as a carbon and nitrogen source. Nitrogen source-dependent enzyme activity, cotranscription, and quantitative gene expression analyses suggest that methylamine metabolism occurs via the GMA/NMG pathway. Sarcosine oxidase (SOX), an NMGDH homolog, was induced by sarcosine, and this allows the growth of strain C5pp on sarcosine as a sole source of carbon and nitrogen. Induction and expression of glutamine synthetase (GS) along with GMAS suggests that both enzymes are involved in the metabolism of methylamine. Taken together, these results demonstrate that methylamine is an important metabolic intermediate and is the source of nitrogen for strain C5pp. Thus, carbaryl serves as the sole source of carbon, nitrogen, and energy for this bacterium and thereby facilitates its degradation.

RESULTS AND DISCUSSION

***Pseudomonas* sp. strain C5pp utilizes carbaryl as a carbon and nitrogen source.** *Pseudomonas* sp. strain C5pp attained maximum growth by 12 h on MSM supplemented with carbaryl as the carbon source and ammonium chloride or ammonium nitrate as the nitrogen source (Fig. 1). On MSM plus carbaryl as the carbon and nitrogen source, growth was delayed by 4 h and the culture entered stationary phase by 16 h (Fig. 1). Strain C5pp failed to grow on MSM plus methylamine as the carbon and nitrogen source. However, it showed growth on glucose as the carbon source and methylamine as the nitrogen source, and the culture entered stationary phase by 8 h (Fig. 1). The strain showed efficient growth on sarcosine as the carbon and nitrogen source and entered stationary phase by 7 h (Fig. 1). These growth profiles suggest that strain C5pp has the ability to utilize carbaryl as a carbon and nitrogen source while

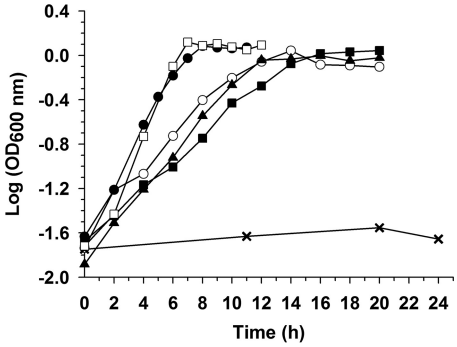

FIG 1 Growth profile of *Pseudomonas* sp. strain C5pp on the combinations of carbon and nitrogen sources. Minimal salt medium was supplemented with (i) carbaryl as a carbon and nitrogen source (■), (ii) carbaryl as a carbon source and ammonium chloride as a nitrogen source (○), (iii) carbaryl as a carbon source plus ammonium nitrate as a nitrogen source (▲), (iv) glucose as a carbon source and methylamine as a nitrogen source (●), methylamine as a carbon source and a nitrogen source (×), and sarcosine as a carbon and nitrogen source (□). The concentration of carbon and nitrogen used was 0.1%. Growth was monitored spectrophotometrically by measuring the optical density at 600 nm (OD_{600}).

methylamine is used only as the nitrogen source. It has been reported that various bacterial species can use methylamine as the sole nitrogen source; this physiological trait indicates that methylamine is an important nitrogen source (6). Nonmethylotrophic organisms like *Bacillus, Pseudomonas,* and *Agrobacterium* are reported to use methylamine as a nitrogen source (5, 6), while methylotrophs utilize it as a carbon as well as a nitrogen source (11, 23). Strain C5pp failed to grow on formaldehyde (0.02, 0.2, 2, 10, and 20 mM) as the carbon source in the presence of methylamine as a nitrogen source.

Gene clusters involved in methylamine and nitrogen metabolism. The genome analyses of strain C5pp revealed the presence of genes encoding putative enzymes and proteins involved in methylamine and nitrogen metabolism (Fig. 2a). Genes encoding enzymes of the γ-glutamylmethylamide/*N*-methylglutamate (GMA/NMG) pathway were found to be present on contigs 15 and 35; ammonium or methylamine transport were found to be present on contigs 1, 15, and 37, while those encoding GS (*glnA*), NADP-dependent glutamate dehydrogenase (NADP-GDH; *gdhA*), NAD-dependent glutamate dehydrogenase (NAD-GDH; *gdhB*), formaldehyde dehydrogenase (FALDH; *adh*), S-formylglutathione hydrolase (FGH; *fghA*), and sarcosine oxidase (SOX; *soxBDAG*) were present on contigs 2, 24, 37, 5, 34, and 8, respectively (Fig. 2a). However, genes for MADH (*mau* cluster) and MAO (*maoxI* and *maoxII*), present in methylotrophs for the utilization of methylamine as a carbon and nitrogen source (7, 23), were absent from the draft genome of strain C5pp.

The arrangement of genes involved in the GMA/NMG pathway from strain C5pp was compared with that of various methylamine-utilizing bacterial isolates (Fig. 2b). Contig 15 in strain C5pp harbored a cluster of five genes (5.72 kbp) putatively coding for an ammonium transporter, NMGS, and GMAS. Contig 35 contained a cluster of six genes (6.85 kbp) putatively encoding NMGDH and enzymes involved in formaldehyde metabolism. However, strain C5pp is unable to grow on formaldehyde as the carbon source. These two gene clusters present on contig 15 and 35 appear to be separated by a distance of at least 37.7 kbp. However, the two clusters reported from other organisms (Fig. 2b) are present as an eight-gene cluster harboring *gltB132-mgsABC, soxBDAG-mgdABCD,* and *gltIII-gmaS* (1, 2). The annotation, putative function, and identity to other similar proteins is given in Table S1 in the supplemental material.

The *mgsABC* locus encodes polypeptides with high identity and clustered with individual domains of glutamate synthase, glutamine amidotransferase (*gltB1*), glutamate synthase subunit α (*gltB3*), and ferredoxin-dependent glutamate synthase (*gltB2*) (Table S1 and Fig. S1a, b, and c). In *Methyloversatilis universalis* FAM5 (*mgsABC*) and *Methylocella silvestris* (*gltB132*), these genes are reported to code for NMGS and are involved in methylamine metabolism (1, 2).

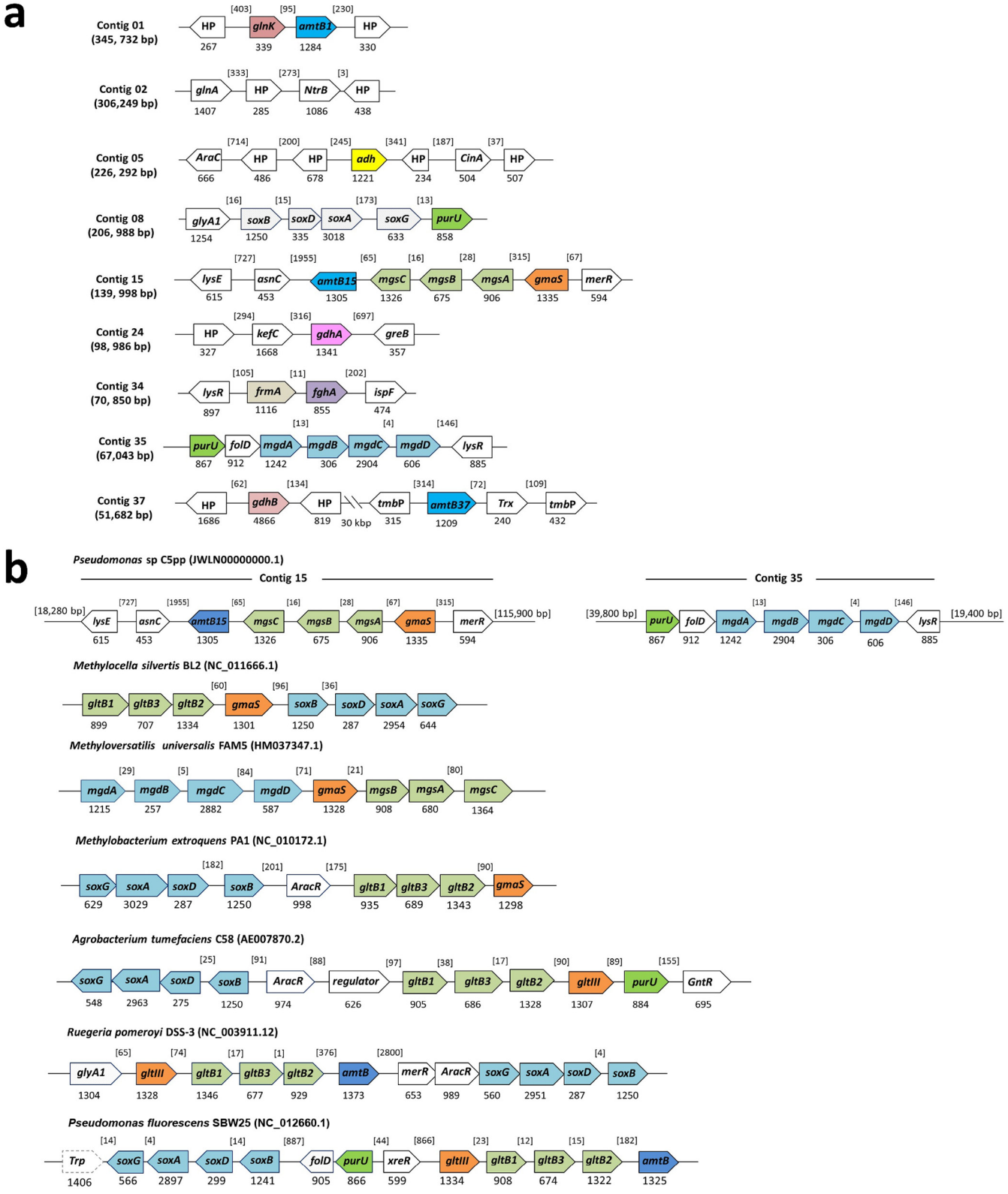

FIG 2 Genetic organization of genes associated with nitrogen metabolism in *Pseudomonas* sp. strain C5pp. (a) The arrangement of genes associated with nitrogen assimilation, methylamine metabolism, formaldehyde detoxification, and sarcosine metabolism in *Pseudomonas* sp. strain C5pp. (b) Comparison of an organization of genes involved in methylamine metabolism from *Pseudomonas* sp. strain C5pp with methylotrophs and nonmethylotrophs. Abbreviations: HP, hypothetical protein; *glnK*, nitrogen regulation protein P-II; *amtB1*, ammonium transporter present on contig 01; *glnA*, glutamine synthetase; *ntrB*, nitrogen regulatory protein; *aracR, asnC, lysR, lysE, xreR,* and *merR*, transcriptional regulators; *adh,* formaldehyde dehydrogenase; *gdh*, glutamate dehydrogenase; *cinA*, CinA domain protein; *glyA1*, serine hydroxymethyltransferase; *soxB*, sarcosine oxidase subunit *β*; *soxD*, sarcosine oxidase subunit *δ*; *soxA*, sarcosine oxidase

(Continued on next page)

gmaS sequence was predicted to code for GMAS (Fig. 2b and Table S1), belonging to the GS family. Sequence analysis of GMAS from strain C5pp indicated that it lacks two key ammonia-binding residues (D50 and S53) that are commonly found in GS (24), while ATP and glutamate binding motifs are conserved (Fig. 3a). Phylogenetic analysis indicates clustering of GMAS from strain C5pp (66% identity) (Table S1) with the functionally characterized GMAS from *Methylovorus mays* (25), while three GS (types I, II, and III) form a separate clade (Fig. 3b). Therefore, the presence of both NMGS and GMAS in strain C5pp suggests that methylamine metabolism occurs via the GMA/NMG pathway.

The gene product of *glnA* (contig 2) from strain C5pp, a putative GS-I (Table S1), contains ammonia-binding residues (D50 and S53) as well as other conserved motifs (Fig. 3a), and it clustered with the functionally characterized GS-I from *Salmonella enterica* (64% identity) (Fig. 3b and Table S1). The analysis suggests that strain C5pp possesses both GS and GMAS, which are likely involved in ammonia assimilation and methylamine metabolism, respectively.

The strain C5pp genome was found to possess three different putative ammonium transporter genes, namely, *amtB1, amtB15,* and *amtB37*, on contigs 1, 15, and 37, respectively (Fig. 2a). Of the three, AmtB15, encoded by a gene in contig 15, is present in the vicinity of GMA/NMG pathway enzymes, and it clustered with the functionally characterized AmtB of *Escherichia coli* (46% identity) and *Saccharomyces cerevisiae* (38% identity) (Fig. S2 and Table S1). Methylamine acts as an analogue of ammonia and can be transported via AmtB (26). In *S. cerevisiae*, AmtB has been functionally identified and reported to transport methylamine as well (27). AmtB1 and AmtB37 from strain C5pp shared 62 and 32% identity, respectively, with AmtB15. AmtB1 was also found to be clustered with the functionally characterized AmtB of *E. coli* and *Saccharomyces cerevisiae* (Fig. S2 and Table S1). Further, *glnK,* which codes for a putative nitrogen regulatory protein, P-II (present upstream of the *amtB1* gene) (Fig. 2a and Table S1), is involved in regulation of nitrogen metabolism under nitrogen-limiting conditions in *Pseudomonas stutzeri* (28). These analyses indicate that strain C5pp possesses both ammonia as well as methylamine transporters.

mgdABCD were predicted to code for NMGDH in strain C5pp (Fig. 2). Phylogenetic analysis suggested the clustering of MgdB and MgdD from strain C5pp with genetically characterized MgdB and MgdD (50 and 63% identity; Table S1) of *Methyloversatilis universalis* FAM5 (Fig. S3), where these proteins are known to be involved in methylamine metabolism via the NMG pathway. In other methylamine-utilizing organisms, like *Methylocella silvestris*, *Methylobacterium extorquens* PA1, *Agrobacterium tumefaciens*, etc., the *soxBDAG* gene cluster is annotated to code for a putative NMGDH (Fig. 2b). Besides the *mgdABCD* cluster on contig 35, strain C5pp was also found to possess the *soxBDAG* gene cluster on contig 8, annotated to code for putative sarcosine oxidase (SOX) (Table S1). The phylogenetic relationship among these proteins is shown in Fig. S3. BLASTp analysis indicated that SOX encoded by *soxBDAG* (contig 8) possesses high sequence identity (Table S1) to the functionally characterized SOX from *Corynebacterium* sp. strain P-1 (29) and *Stenotrophomonas maltophilia* (30) compared to the NMGDH sequence (contig 35). Hence, to distinguish them from NMGDH, these genes were labeled *soxBDAG*. In addition, *glyA1*, annotated as a putative serine-hydroxymethyltransferase (SHMT), was found to be present upstream of *soxBDAG* and was considered part of the *sox* operon (31). These results indicate that in strain C5pp, methylamine

FIG 2 Legend (Continued)
subunit α; *soxG*, sarcosine oxidase subunit γ; *purU*, formyltetrahydrofolate deformylase; *amtB15*, ammonium transporter present on contig 15; *mgsABC*, *N*-methylglutamate synthase subunits A, B, and C; *gmaS*, γ-glutamylmethylamide synthetase; *kefC*, glutathione-regulated potassium efflux system protein; *gdhA*, NADP-specific glutamate dehydrogenase; *greB*, transcription elongation factor GreB-related protein; *frmA*, *S*-(hydroxy)-methylglutathione dehydrogenase; *fghA*, *S*-formylglutathione hydrolase; *ispF*, 2-C-methyl-D-erythritol 2,4-cyclodiphosphate; *folD,* methylenetetrahydrofolate dehydrogenase/cyclohydrolase; *mgdABCD*, *N*-methylglutamate dehydrogenase subunits A, B, C, and D; *gdhB*, NAD-specific glutamate dehydrogenase; *tmbP*, probable transmembrane protein; *amtB37*, ammonium transporter present on contig 37; *trx*, thiol-disulfide isomerase and thioredoxins; *gltB1*, glutamine amidotransferase; *gltB2*, glutamate synthase large chain; *gltB3*, glutamate synthase putative GlxC; and *gntR*, regulator of gluconate (Gnt) operon. Gene size (in bp) is given below each gene box. Numbers in parentheses indicate the intergenic distance (in bp). The same color represents homologous genes. The accession numbers are given in parentheses.

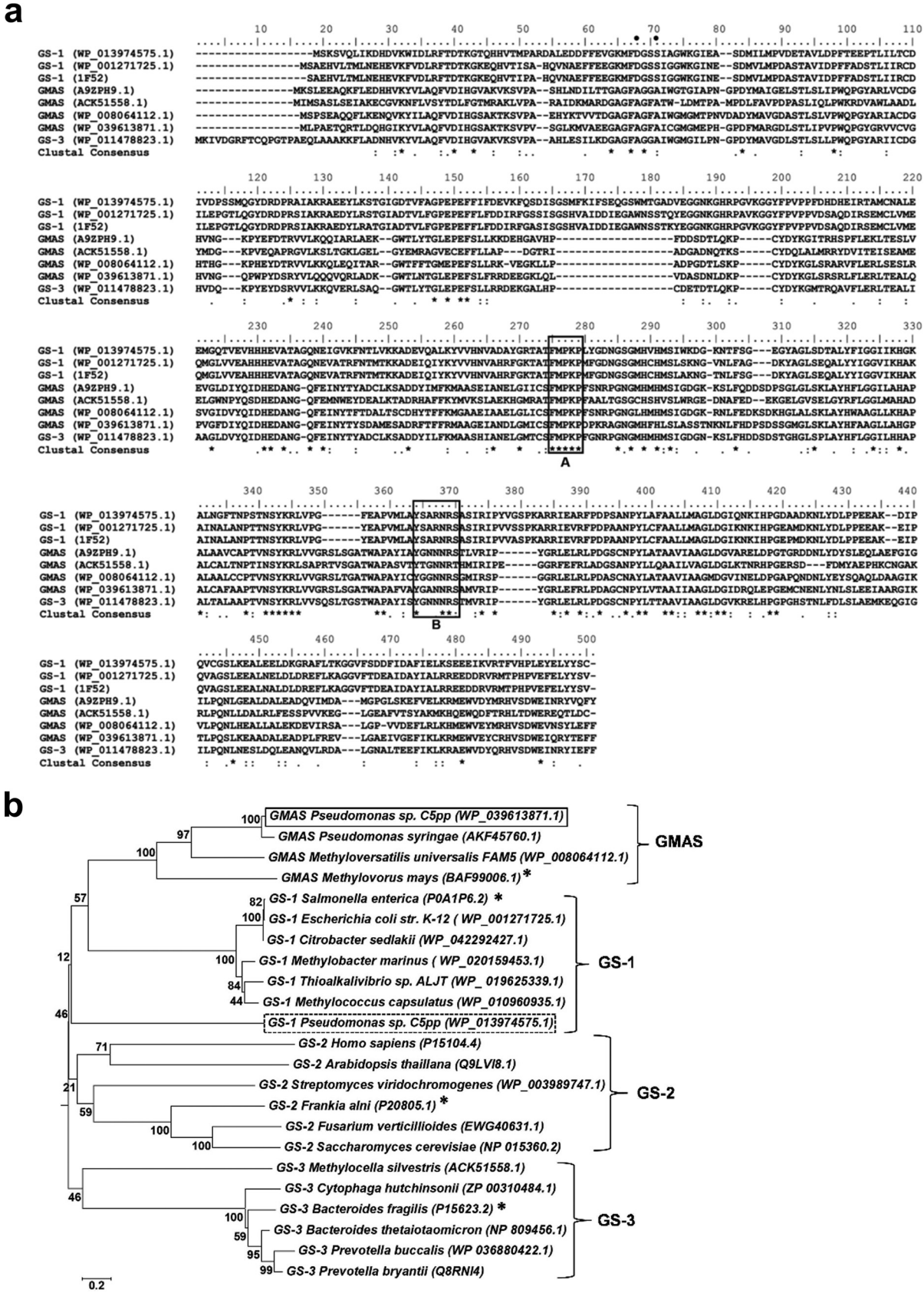

FIG 3 Multiple-sequence alignment and phylogenetic analysis of GS and GMAS from *Pseudomonas* sp. strain C5pp. (a) Sequence alignment of glutamine synthetases (GS-I, -II, and -III) and GMAS amino acid sequences. Strains included the GS-I *Pseudomonas* sp. strain C5pp

(Continued on next page)

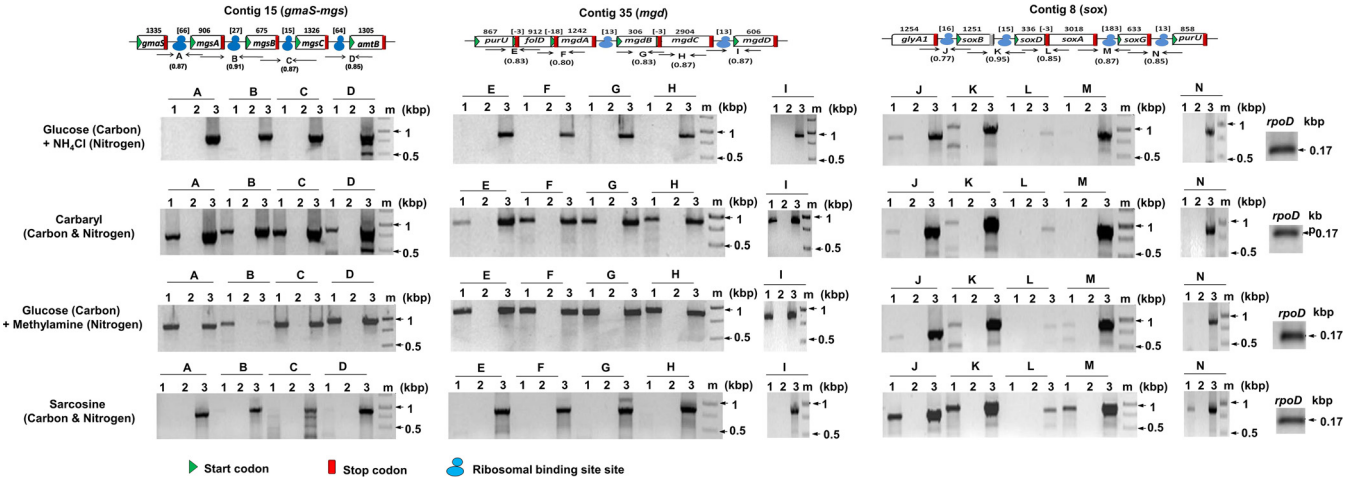

FIG 4 Schematic representation and cotranscriptomic analysis of genes involved in methylamine and sarcosine metabolism in *Pseudomonas* sp. strain C5pp. The arrangement of genes involved in the metabolism of methylamine (contig 15 and contig 35) and sarcosine (contig 8) is shown. The numbers indicate the gene length (bp), numbers in parentheses indicate the intergenic distance (bp), negative signs indicate that the genes are overlapping, and putative promoters identified using BPROM are indicated by −10 and −35 sequences. Agarose gel profiles showing RT-PCR product amplification. PCR amplifications of targeted genes from cDNA synthesized from *Pseudomonas* sp. strain C5pp cells grown on glucose, methylamine, carbaryl, and sarcosine. The arrow designates primer positions (Table 3), and the number indicates the expected length of the PCR product (kbp). Numbers above the lanes refer to amplification conditions: 1, RT-PCR products from total RNA; 2, PCR products from total RNA without RT (reverse transcriptase); 3, PCR products from total genomic DNA of strain C5pp. m, DNA ladder. The expression profile of a housekeeping gene, *rpoD* (0.17 kbp), was taken as an internal reference.

metabolic genes were clustered as *gmaS-mgs* and *mgd,* while those involved in sarcosine metabolism were found in the *sox* cluster.

Nitrogen-dependent cotranscription and induction of *gmaS-mgs*, *mgd*, and *sox* clusters. Detailed bioinformatic analyses of the *gmaS-mgs*, *mgd,* and *sox* clusters revealed the presence of putative −10 and −35 promoter regions, the ribosomal binding site, and start and stop codons in the upstream region of *gmaS-mgsABC-amtB* (~5.7 kbp), *purU-folD-mgdABCD* (~7 kbp), and *glyA1-soxBDAG-folD* (~7.4 kbp) (Fig. 4). Results of reverse transcription-PCR (RT-PCR) using cDNA prepared from cells grown with the different combinations of carbon and nitrogen sources as the template and overlapping gene-specific primers are shown in Fig. 4. Carbaryl-grown cells showed the expected size of RT-PCR product amplification, including intergenic regions for *gmaS-mgs* and *mgd* clusters, indicating that these genes were cotranscribed as two different polycistronic mRNAs, and genes in these clusters are arranged as two independent operons. Attempts to obtain large-size PCR products encompassing either all or at least three genes from these clusters were unsuccessful. This could be due to the instability of mRNA or partial cDNA synthesis. cDNA prepared from carbaryl-grown cells did not show any amplification for the *sox* cluster (Fig. 4). A similar trend was observed for the cDNA prepared from cells grown on glucose plus methylamine (Fig. 4), while sarcosine-grown cells showed amplification of genes present in the *sox* cluster alone. The cDNA prepared from cells grown on glucose plus ammonium chloride did not show RT-PCR products for any of these gene clusters (Fig. 4). These results suggest that irrespective of the carbon source, methylamine induces the transcription of genes located in the *gmaS-mgs* and *mgd* clusters, while sarcosine induces the expression of the *sox* cluster

FIG 3 Legend (Continued)
(WP_013974575.1), *Escherichia coli* (WP_001271725.1), and *Salmonella enterica* serovar Typhimurium (1F52_A) and the GMAS *Pseudomonas* sp. strain C5pp (WP_039613871.1), *Methylovorous mays* (A9ZPH9.1), *Methylocella silvestris* (ACK51558.1), *Methyloversatilis universalis* FAM5 (WP_008064112.1), and *Methylobacillus flagellatus* (WP_011478823.1). Ammonia-binding residues (D50 and S53) in glutamine synthetase are represented by black filled circles. Glutamate and ATP-binding domains are represented by square boxes A and B, respectively. Conserved residues are indicated by asterisks. Protein sequences were retrieved from the NCBI protein database, with accession numbers indicated in parentheses. (b) Phylogenetic tree showing the relationship between glutamine synthetases (GS-I, -II, and -III) and γ- GMAS. Protein sequences were retrieved from the NCBI protein database, with accession numbers indicated in parentheses, and aligned using the ClustalW program. The phylogenetic tree was constructed by using MEGA6 software with the neighbor-joining method (500 bootstrap replicates). Asterisks indicate that proteins are characterized at the functional level.

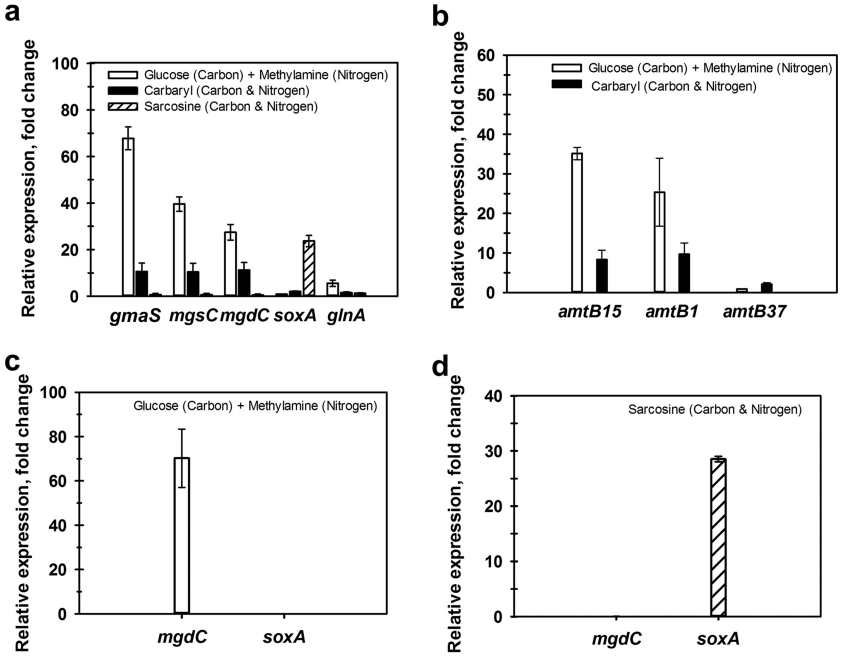

FIG 5 Relative expression of genes involved in methylamine and sarcosine metabolism from *Pseudomonas* sp. strain C5pp under carbon- and nitrogen-limiting conditions. (a) Expression analysis of *gmaS*, *mgdC*, *mgsC soxA,* and *glnA,* encoding γ-glutamylmethylamide synthetase, *N*-methylglutamate dehydrogenase subunit C, *N*-methylglutamate synthase subunit C, sarcosine oxidase subunit α, and glutamine synthetase, respectively, from *Pseudomonas* sp. strain C5pp cells grown on different carbon and nitrogen sources. (b) *amtB1*, *amtB15,* and *amtB37*, encoding putative ammonium and methylamine transporters. (c) *mgdC* and *soxA* from cells grown on glucose plus methylamine. (d) *mgdC* and *soxA* from cells grown on sarcosine as a carbon and nitrogen source. Relative expression was calculated by taking the expression of a housekeeping gene, *rpoD*, as an internal reference.

only. In the presence of ammonium chloride, none of the genes from these clusters were expressed. This operonic arrangement is different from the one in *Methylocella silvestris*, where eight genes encoding GMAS, NMGS, and NMGDH are arranged together as a single operon that is induced by methylamine (2). However, this is similar to *Methylobacterium extorquens*, where *mgs-gmaS* and *mgd* were found to be induced by methylamine as two divergent gene clusters (10).

The quantification of gene expression (quantitative PCR [qPCR]) analyses of *gmaS* (GMAS), *mgsC* (NMGS), *mgdC* (NMGDH), and *soxA* (SOX) representatives of *gmaS-mgs*, *mgd*, and *sox* clusters, *glnA* (GS), and three *amtB* genes (ammonium transporter) under various conditions was performed, and results are depicted in Fig. 5. Compared to expression in cells grown in glucose and ammonium chloride, the relative (fold) expression of *gmaS* (67), *mgsC* (39), *mgdC* (27), and *glnA* (5.6) was found to be highest in cells grown in glucose plus methylamine and lowest in sarcosine-grown cells. However, the carbaryl-grown cells showed intermediate-level expression of these genes (*gmaS, mgsC,* and *mgdC,* ~10- to 11-fold; *glnA,* 1.5-fold) (Fig. 5a). *soxA* showed 24-fold higher expression in sarcosine-grown cells than under other conditions (Fig. 5a). These results indicate that in strain C5pp, genes at *gmaS-mgs*, *mgd*, and *sox* clusters, which are transcribed as a polycistronic mRNA, are induced by respective, specific nitrogen sources.

Relative expression analysis for genes encoding ammonia transporters showed that, compared to that of cells grown in glucose plus ammonium chloride, the cells grown in glucose plus methylamine exhibited maximum expression of *amtB15* (35-fold) and *amtB1* (25-fold) (Fig. 5b). However, the expression of *amtB37* was found to be significantly lower. The expression observed from cells grown on carbaryl as a carbon and nitrogen source was moderate (9- to 10-fold) for *amtB15* and *amtB1*. This difference could reflect the effective concentration of methylamine generated. From carbaryl as a

TABLE 1 Activity of various enzymes of methylamine metabolic pathway from *Pseudomonas* sp. strain C5pp cells grown on different combinations of carbon and nitrogen sources

Enzyme[a]	Sp act (nmol·min^{-1}·mg^{-1}) of cells grown on:			
	Carbaryl (C and N)	Glucose (C) + methylamine (N)	Glucose (C) + NH_4Cl (N)	Carbaryl (C) + NH_4Cl (N)
NMGDH	7.4 ± 1.4	11.2 ± 3.2	ND[b]	ND
GMAS	83.8 ± 23.0	150.8 ± 32.0	6.65 ± 0.2	3.3 ± 1.2
FALDH	215.0 ± 9.0	225.0 ± 8.0	45.3 ± 7.0	53.0 ± 3.0
GS	80.7 ± 8.0	158.3 ± 25.0	11.3 ± 3.2	6.2 ± 1.6
GDH	12.0 ± 2.3	32.0 ± 1.0	541.0 ± 53.0	224.0 ± 4.0

[a]Enzyme abbreviations: NMGDH, *N*-methylglutamate dehydrogenase; GMAS, γ-glutamylmethylamide synthetase; FALDH, formaldehyde dehydrogenase; GS, glutamine synthetase; GDH, glutamate dehydrogenase.
[b]ND, not determined.

nitrogen source, a 6-fold lower concentration of methylamine (5 mM) will ensue compared to that with methylamine as the nitrogen source (32 mM). AmtB15, AmtB1, and AmtB37 were predicted to be located in the inner membrane (Fig. S4). *amtB15* was found to be a part of the *gmaS-mgs* cluster and was cotranscribed with the genes encoding methylamine-metabolizing pathway enzymes (Fig. 4). These results suggest that carbaryl and methylamine induce expression of *amtB15* and *amtB1*, which encode transporters involved in methylamine metabolism.

To establish the involvement of the *mgd* cluster and not the *sox* cluster in methylamine metabolism, qPCR was performed for cells grown on glucose plus methylamine or sarcosine. Results are shown in Fig. 5c and d. In cells grown in glucose plus methylamine, expression of *mgdC* was significantly higher than that of *soxA* (Fig. 5c). However, *soxA* showed maximum expression compared to that of *mgdC* in sarcosine-grown cells (Fig. 5d). These results indicate that genes encoding putative SOX and NMGDH are present on contigs 8 and 15, respectively, and are induced by respective nitrogen sources.

Nitrogen-dependent induction of enzymes. The activity of various enzymes involved in the GMA/NMG pathway as well as in ammonia assimilation was monitored from cells grown on various combinations of carbon and nitrogen sources, and the results are depicted in Table 1. The following important observations were made. (i) With respect to the GMA/NMG pathway, compared to carbaryl as the nitrogen source, the activities for GMAS and NMGDH were ~2-fold higher in glucose plus methylamine as the carbon and nitrogen source; however, these activities were very low in the presence of ammonium chloride as the nitrogen source (Table 1). The activity of FALDH also was found to be 5-fold higher when carbaryl or methylamine was used as a nitrogen source than when ammonium chloride was used as the nitrogen source (Table 1). Similar enzyme activity trends were reported from *M. silvestris*, wherein methylamine-grown cells showed the higher activity of GMAS and NMGDH as well as higher production of formaldehyde compared to that of cells grown in methanol plus ammonia (2). Formaldehyde is further metabolized as a carbon source by methylotrophs, while nonmethylotrophs will oxidize it to CO_2 (3). Formaldehyde, formed as an end product of methylamine metabolism, was oxidized to carbon dioxide by FALDH in strain C5pp, and this strain failed to grow on methylamine (or formaldehyde) as the carbon source. (ii) With respect to the ammonia assimilation pathway, the activity of GS was significantly higher from cells grown on carbaryl or methylamine than from those grown on ammonium chloride as a nitrogen source. Further, 2-fold higher GS activity was observed from cells grown on glucose plus methylamine than from cells grown on carbaryl (Table 1). In addition, the activity of GDH was significantly higher in the cells grown on ammonium chloride than on carbaryl or methylamine as a nitrogen source. Maximal GDH activity was observed in cells grown on glucose plus ammonium chloride. Altogether, these results suggested that in strain C5pp, methylamine generated from carbaryl is metabolized as a nitrogen source via the GMA/NMG pathway, and ammonia released is assimilated through the GS/GOGAT pathway. It was observed that in *Methylobacterium extorquens* AM1 (previously referred to as *Pseudomonas* sp. strain

AM1), methylamine used either as a carbon or nitrogen source via the GS-GOGAT pathway is followed for nitrogen assimilation. However, when ammonia is used as a nitrogen source, the organism possesses an NADPH-dependent GDH for its assimilation (32).

GMAS and GS are two different proteins. GS is a key enzyme in nitrogen metabolism. It catalyzes the conversion of glutamate and ammonia to glutamine and plays a crucial role in amino acid metabolism. Some GS and GS-like enzymes also accept other amine donors in place of ammonia (e.g., methylamine, isopropylamine, etc.). Examples of some such reactions include the production of GMA from glutamate and methylammonium (33). Few methylamine-utilizing bacteria are known to convert methylamine into GMA in the presence of glutamate by GMAS, and this plays a role in methylamine metabolism.

Methylamine-utilizing strain C5pp was found to possess both GS and GMAS. The activity of both of the enzymes was found to be almost similar to that of the cell extract (CFE) of strain C5pp cells grown on carbaryl or methylamine as the nitrogen source (1:1 ratio) (Table 1). Reactions catalyzed by both GMAS and GS are very similar (catalyzing the formation of glutamine and GMA), because of which it was difficult to differentiate among them. Therefore, a separation and partial purification of GS and GMAS from the cells grown on glucose plus methylamine was attempted using DEAE ion-exchange chromatography. The peak activities of GMAS and GS were eluted in the same fractions (Fig. S5). The question remains as to whether strain C5pp possesses two distinct enzymes (one GMAS and the other a GS) or both reactions are catalyzed by a single enzyme of broad substrate specificity. However, the draft genome of strain C5pp has two genes (*glnA* and *gmaS*) present on different contigs, 2 and 15 (Fig. 2a). To investigate in detail, both GMAS (Fig. 6a) and GS (Fig. 6b) from strain C5pp were cloned separately into pET vector and expressed in *E. coli*. The soluble protein fraction (Fig. 6a) of recombinant GMAS (rGMAS) did not show any activity with hydroxylamine or *N*-methylhydroxylamine. Further, various additives, like glutamate, magnesium sulfate, β-mercaptoethanol, and glycerol, either alone or in combination, were added during enzyme induction or CFE preparation in order to stabilize the activity. Although protein was found to be expressed under all of these conditions, the rGMAS activity could not be detected, suggesting that expressed soluble protein is inactive.

The soluble fraction of *E. coli* cells expressing recombinant GS_{C5pp} (rGS_{C5pp}) showed activity on both substrates, i.e., hydroxylamine (2.22 ± 0.12 μmol·min^{-1}·mg^{-1}) and *N*-methylhydroxylamine (1.52 ± 0.08 μmol·min^{-1}·mg^{-1}). The expressed rGS_{C5pp} was purified using nickel-nitrilotriacetic acid (Ni-NTA) chromatography (Fig. 6c). The purified rGS_{C5pp} also acted on both substrates and displayed a weak substrate inhibition with hydroxylamine (ammonia analogue) as the substrate (Fig. 6d). However, it displayed strong substrate inhibition with *N*-methylhydroxylamine (Fig. 6e, methylamine analogue) compared to that with hydroxylamine. Various kinetic constants determined for rGS_{C5pp} are summarized in Table 2. The enzyme showed higher affinity for hydroxylamine (ammonia analogue, 6.13 ± 1.35 mM) than *N*-methylhydroxylamine (methylamine analogue, 26.32 ± 7.59 mM), indicating that hydroxylamine is its actual substrate but can also act on methylamine to yield GMA. Earlier, GS and GMAS from *Pseudomonas* sp. strain MS were purified, and it has been reported that GMAS was more specific for GMA (34). The ability of GS to act on both substrates was also reported for *Methylovorus mays* (25). For the sake of comparison, GS from an *E. coli* host was cloned into pET vector, overexpressed, and purified by Ni-NTA column chromatography (Fig. S6a and b). The purified recombinant *E. coli* GS (rGS_{Ec}) was found to act on both substrates as well as display substrate inhibition with both hydroxylamine (Fig. S6c) and *N*-methylhydroxylamine (Fig. S6d). However, *N*-methylhydroxylamine (with a K_m of 60.2 ± 2.2 mM) was a significantly less effective substrate for rGS_{Ec} than hydroxylamine (K_m, 14.85 ± 1.34 mM). Altogether, these results suggest that GS from *Pseudomonas* strain C5p possesses higher catalytic efficiency (k_{cat}/K_m, 1.02 s^{-1} mM^{-1}) for substrate *N*-methylhydroxylamine than *E. coli* GS (k_{cat}/K_m, 0.42 s^{-1} mM^{-1}) (Table 2).

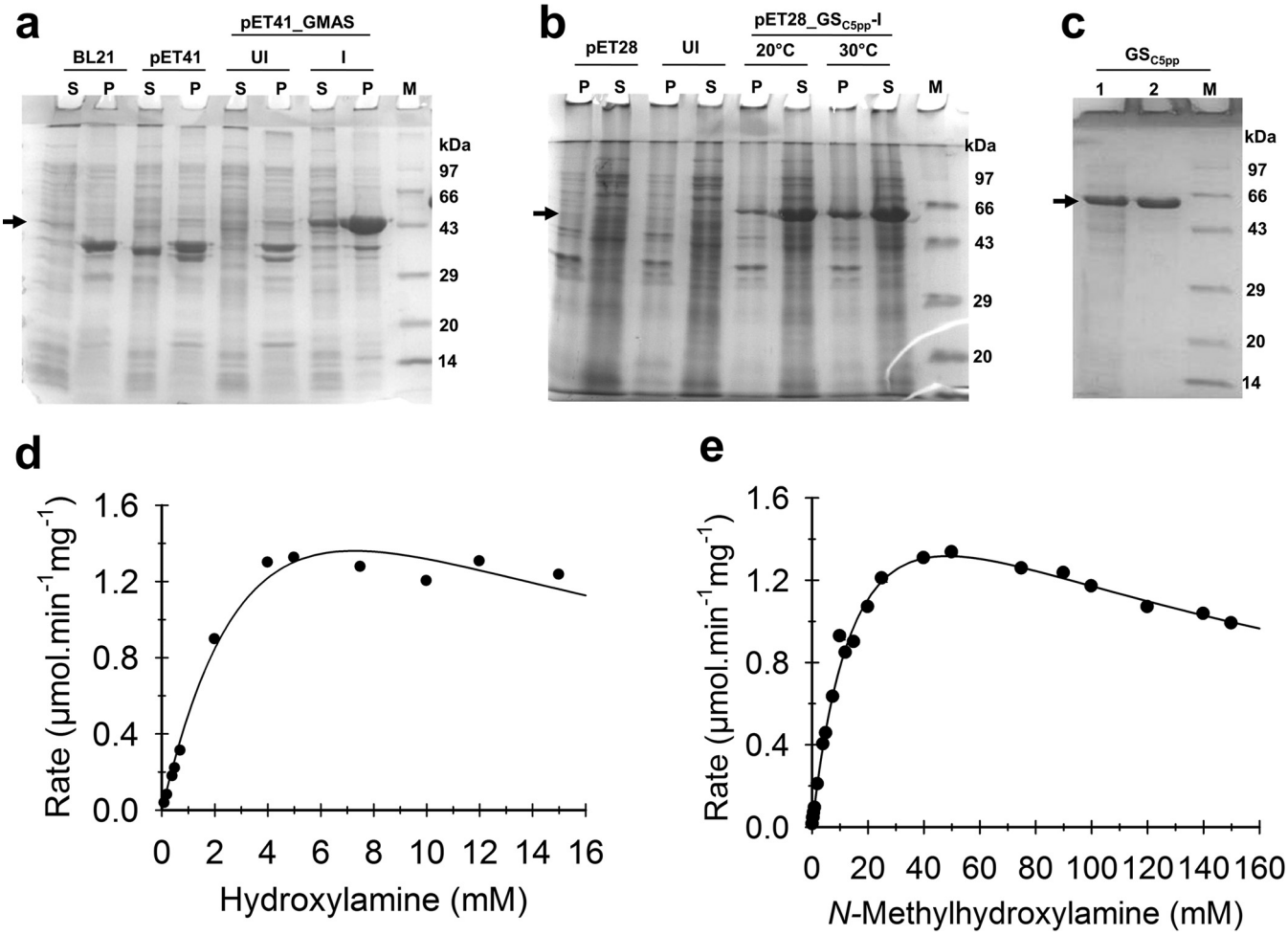

FIG 6 SDS-PAGE profile of recombinant GMAS and glutamine synthetase (GS_{C5pp}), substrate saturation profile of recombinant GS_{C5PP}, and kinetic properties of recombinant GS_{C5pp}. (a) SDS-PAGE analysis of GMAS from strain C5pp expressed into *E. coli*. Induction was carried out using IPTG (100 μM) at 20°C for 17 h in *E. coli*. (b) GS_{C5PP} induction was carried out using IPTG (100 μM) at 20°C and 30°C for 16 h and 6 h, respectively. In panels a and b, BL21 represents *E. coli* BL21 cells without vector and genes of interest, pET28 and pET41 represent BL21 cells carrying vector alone, P denotes pellet or insoluble fraction, S denotes supernatant or soluble fraction, and UI and I represent uninduced and induced. (c) SDS-PAGE analysis of protein eluted during the purification of recombinant GS_{C5PP} from *E. coli* cells. Lane 1, cell extract; 2, Ni-NTA-purified enzyme. In panels a, b, and c, lane M denotes the protein molecular mass markers (in kDa). Phosphorylase B, 97.4 kDa; BSA, 66 kDa; ovalbumin, 43 kDa; carbonic anhydrase, 29 kDa; soybean trypsin inhibitor, 20.1 kDa; lysozyme, 14.3 kDa. An arrow indicates the GMAS and GS of sizes ~49 and ~53 kDa, respectively. (d and e) Substrate saturation plots of GS_{C5PP} for substrate hydroxylamine (d) and *N*-methylhydroxylamine (e).

Generally, GMA is considered an essential intermediate and GMAS a biomarker in methylamine metabolism (2, 11). Although an active rGMAS enzyme could not be demonstrated, the putative gene encoding GMAS was expressed and induced by methylamine in strain C5pp. Our results suggest that both GMAS and GS are required when methylamine is utilized as a nitrogen source by strain C5pp.

In conclusion, the presence of the methylamine oxidation pathway for its metabolism as a carbon, nitrogen, and/or energy source would confer some advantage to the microbes, considering that many environments are often limited by the availability of carbon and inorganic nitrogen sources. This study describes the physiological significance of methylamine metabolism in the carbaryl-degrading strain C5pp. The proposed metabolic pathway for the utilization of carbaryl as the carbon and nitrogen source is depicted in Fig. 7. Methylamine derived from carbaryl in the periplasm is transported into the cytoplasm by putative AmtB across the inner membrane and metabolized as a nitrogen source via an inducible cytosolic GMA/NMG pathway. The ammonium generated during methylamine metabolism can be assimilated as a nitrogen source via the GS-GOGAT pathway and allows strain C5pp to grow on carbaryl as a sole source of

TABLE 2 Kinetic properties of recombinant GS from *Pseudomonas* sp. strain C5pp and *Escherichia coli*[c]

Parameter	Value for:			
	GS_{C5pp}		GS_{Ec}	
	Hydroxylamine	*N*-Methylhydroxylamine	Hydroxylamine	*N*-Methylhydroxylamine
K_m (mM)[a]	6.13 ± 1.35	26.32 ± 7.59	14.85 ± 1.34	60.15 ± 2.19
V_{max} (μmol·min^{-1}·mg^{-1})	3.58 ± 0.62	2.53 ± 0.62	7.6 ± 0.28	2.4 ± 1.27
K_i (mM)	10.53 ± 3.61	93.63 ± 23.51	3.0	66.85 ± 19.8
k_{cat} (s^{-1})[b]	37.89	26.87	80.56	25.44
k_{cat}/K_m (s^{-1} mM^{-1})	6.19	1.02	5.42	0.42

[a]Hydroxylamine and *N*-methylhydroxylamine were used as analogues of ammonia and methylamine, respectively. For details, see the Materials and Methods.
[b]To calculate k_{cat}, the enzyme was considered to possess 12 identical subunits in both cases, i.e., *Pseudomonas* sp. strain C5pp and *E. coli*.
[c]Activity was monitored using the assay described in Materials and Methods, except that the reaction buffer used was 50 mM imidazole-HCl, pH 8.0 (optimum pH), and incubation time was 60 min.

carbon and nitrogen. The compartmentalization of the carbaryl degradation pathway as the localization of enzymes such as CH in the periplasm and lower pathway enzymes (1NH, GDO, etc.), along with methylamine metabolic pathway enzymes in the cytosol, suggests the adaptation of strain C5pp to the toxic carbaryl-contaminated environment. Overall, the environmental conditions, such as accumulation of toxic xenobiotics and carbon/nitrogen source preference, determine the adaptation of an organism for its survival in the toxic environment. Strains like C5pp are valuable for eliminating environmental contaminants like carbaryl efficiently as well as for maintaining biogeochemical cycles.

MATERIALS AND METHODS

Bioinformatic analyses. A sequence-based analysis (BLASTp) (35) was performed to identify genes involved in methylamine and nitrogen metabolism using the available genome sequence of *Pseudomonas* sp. strain C5pp (accession no. JWLN00000000.1) (15). The promoter regions were identified using a bacterial promoter prediction tool, BPROM (Softberry, Inc., Mount Kisco, NY, USA). The phylogenetic tree was constructed for similar proteins/enzymes (annotated as well as functionally characterized) obtained from NCBI BLAST using the neighbor-joining (NJ) algorithm by using Molecular Evolutionary Genetics Analysis, version 6.0 (MEGA6). The robustness of the tree topology was assessed by bootstrap analysis of 500 replicons using the Jones-Taylor-Thornton (JTT) model (36). The topology of putative ammonia transporter protein was predicted by using the Protter server (37).

Cultures and growth conditions. Strain C5pp was grown on minimal salt medium (MSM) (19) supplemented aseptically with appropriate carbon (0.1%, wt/vol) and nitrogen (0.1%, wt/vol) sources. The combinations were (i) carbaryl as carbon source and nitrogen source, (ii) carbaryl as carbon source and ammonium chloride as nitrogen source, (iii) carbaryl as carbon source and ammonium nitrate as nitrogen source, (iv) methylamine as carbon and nitrogen source, (v) glucose as carbon source and methylamine as nitrogen source, and (vi) sarcosine as carbon and nitrogen source. Growth was monitored by measuring the optical density at 600 nm (OD_{600}) spectrophotometrically (Lambda 35; Perkin Elmer, USA). *Escherichia coli* strains DH5α and BL21(DE3), used in this study, were grown in Luria-Bertani broth (38) with or without antibiotic (kanamycin, 40 μg·ml^{-1}).

Cotranscription and relative gene expression (qPCR) analyses. Strain C5pp cells grown on a combination of carbon and nitrogen sources (up to an OD_{600} of 0.8) were processed for total RNA isolation using an RNeasy protect bacteria minikit per the manufacturer's instructions (Qiagen, Germany). Traces of DNA contamination were eliminated by treating the preparation with DNase I (2 U; Invitrogen, USA). The quantification of RNA was performed using a microplate reader (Multiskan Go; Thermo Fisher, USA). cDNA synthesis was performed per the manufacturer's protocol (Invitrogen, USA) using DNA-free RNA (1 μg) as a template.

Cotranscription analysis was performed using endpoint PCRs with cDNA as a template and gene-specific primers (Table 3). In negative controls, the template used was the cDNA preparation with RNase treatment and/or lacking reverse transcriptase. The genomic DNA of strain C5pp as a template was used as a positive control.

For quantitative gene expression analysis, qPCR reactions were performed using the PowerUp SYBR green qPCR MasterMix (Invitrogen, Thermo, USA) with StepOnePlus real-time PCR (Applied Biosystems, USA) per the manufacturers' protocols. Each qPCR reaction mixture (final volume, 20 μl) contained cDNA (4 μl of 10 ng) prepared from cells (OD_{600} of 0.8) grown under different combinations of carbon and nitrogen sources and 500 nM (each) gene-specific forward and reverse primer (Table 3). The thermal cycling program was initial denaturation at 50°C for 2 min, followed by 95°C for 10 min and 40 cycles of amplification, wherein each cycle was comprised of denaturation at 95°C for 15 s and annealing and extension at 60°C (*gmaS*, *amtB1*, *amtB15*, and *amtB37*) or 65°C (*rpoD*, *glnA*, *mgdD*, *soxA*, and *mgsC*) for 1 min. The expression of a housekeeping gene, *rpoD* (σ^{70} transcription factor), was taken as an internal reference. The expression levels of target genes from cells grown on glucose, carbaryl, methylamine, or sarcosine were determined by the cycle value at which

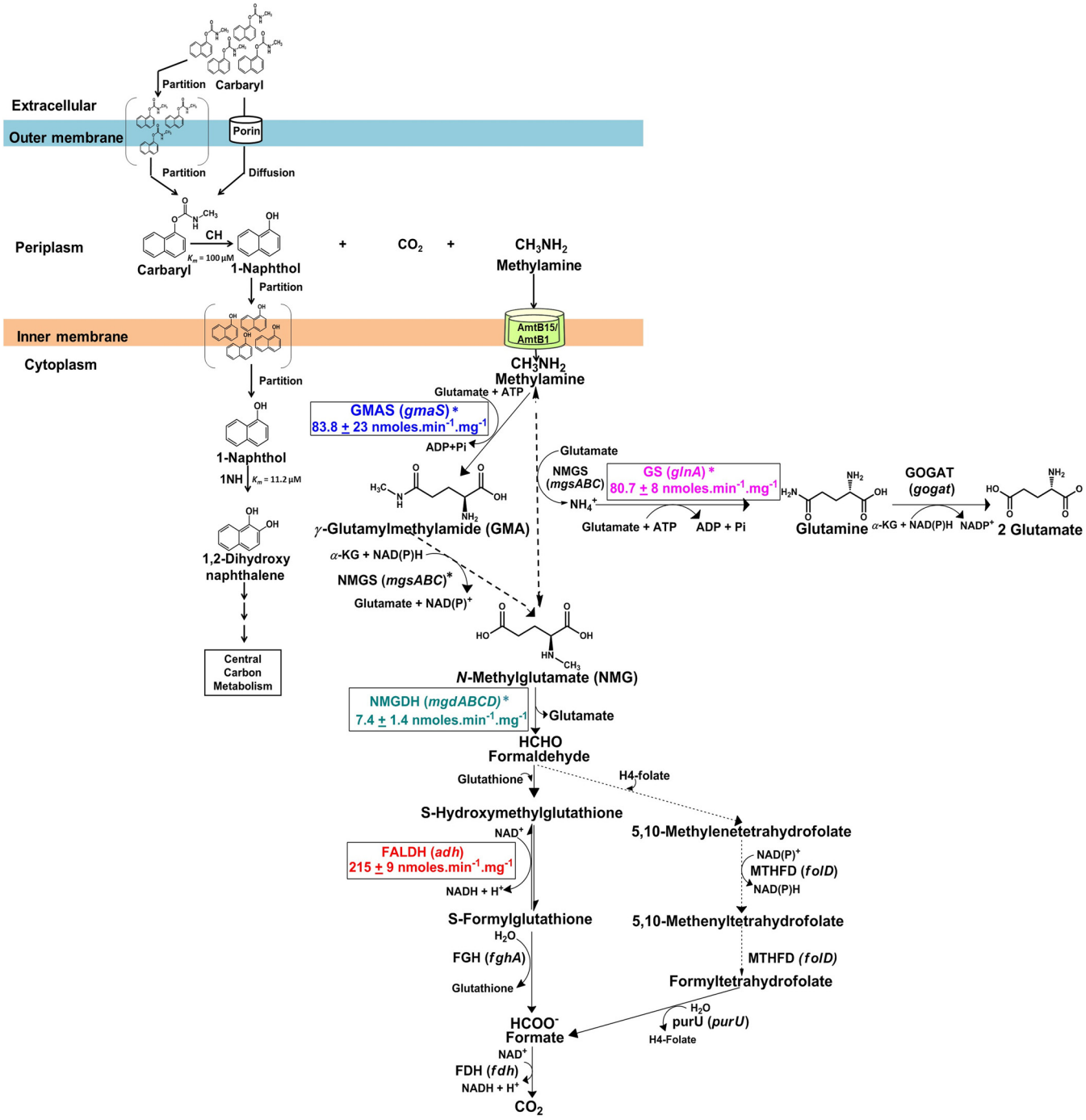

FIG 7 Proposed pathway for the complete utilization of carbaryl as the carbon and nitrogen source in *Pseudomonas* sp. strain C5pp. The genes are depicted in italics. The measured specific activity (nmol·min^{-1}·mg^{-1}) for various enzymes is shown in the box. An asterisk indicates that the relative expression of genes was monitored from carbaryl-grown *Pseudomonas* sp. strain C5pp cells. Dashed and dotted lines represent the possible routes for methylamine oxidation and formaldehyde detoxification in *Pseudomonas* sp. strain C5pp.

fluorescence of the genes of interest cross threshold levels (C_T). ΔC_T was calculated by the equation $\Delta C_T = C_{T(\text{target gene})} - C_{T(rpoD)}$. Gene expression under different growth conditions was compared using the equation $\Delta\Delta C_T = \Delta C_{T(\text{carbaryl/methylamine/sarcosine})} - \Delta C_{T(\text{glucose})}$ (39). Values from at least two or three independent experiments, wherein reactions were performed in duplicate, were used to calculate ΔC_T. All PCR products obtained from the cotranscription and qPCR reactions were gel purified and sequence confirmed (Bencos, India, and First Base, ASP, India).

Enzyme assays. Strain C5pp cells grown on various combinations of carbon and nitrogen sources until late-log phase were harvested by centrifugation, washed, and resuspended (1 g cells in 5 ml buffer) in ice-cold potassium-phosphate buffer (50 mM, pH 7.5). Cells were disrupted by sonication (6 cycles;

TABLE 3 Primers used in this study

Region and primer name	Sequence (5′ to 3′)[a]	Product size (kbp)
Primers for cotranscriptional analysis, RT-PCR		
gmaS-mgsA		
A_RT F	ACCTCTACAACCTGAGCCTGG	0.87
A_RT R	CTTGAGCTCCTGGCGCAG	
mgsA-mgsB		
B_RT F	GAGCATCGAGATCCTCAAG	0.91
B_RT R	TCACCCTCGATCACCAGC	
mgsB-mgsC		
C_RT F	ACGGCAAGCACAACCTGG	0.87
C_RT R	TCATGCCGGCGATAGTCAC	
mgsC-amtB		
D_RT F	ATCGAGCACGTCGGCATC	0.85
D_RT R	AGCTGTCATGGCCGATGTC	
purU-folD		
E_ RT F	AGATCCTCTCCGACGACCTG	0.83
E_RT R	ACCACCACCGCATGCTTG	
folD-mgdA		
F_RT F	TTCCACAGCGAGAACGTC	0.80
F_RT R	TCGTTCGACAGGTTCTGGAAC	
mgdA-mgdB		
G_RT F	ATCCGAAATGGCCGCATC	0.83
G_RT R	TCGGCCAGGAACCAGTAGC	
mgdB-mgdC		
H_RT F	TTCAGGCACATGCCCGAC	0.87
H_RT R	ATGTCGAAGCGGGCGTAG	
mgdC-mgdD		
I_RT F	TGATCATCAGCCAGGACAC	0.87
I_RT R	CACATTCAGCACGATCACG	
glyA1-soxB		
J_RT F	TTCAAGGTCGCTCAGTGC	0.77
J_RT R	ATCACTTCGGTCTGCTGG	
soxB-soxD		
K_RT F	ACCTGGATTGCTCGAAGAACAC	0.95
K_RT R	TGAATACCGCGTGGGTTG	
soxD-soxA		
L_RT F	GCATATTTTCTGTCCCCACTGC	0.85
L_RT R	ACGATCAGCACGTCGCAG	
soxA-soxG		
M_RT F	ATGAACCGCGAAGACTGC	0.87
M_RT R	TGACATTGACCACCACCTGGATG	
soxG-purU		
N_RT F	GCGTAACCCTGCGTGAAC	0.85
N_RT R	ATACAGCAGGTCGTTAAGGCAG	
Primers for qPCR		
rpoD		
*rpoD*_RT F	ATCGAGGAAGGCATCCGTG	0.17
*rpoD*_RT R	ATCGGCACTTCTTCGGTCG	
amtB1		
*amtB1*_RT F	ATGACCATTCCGGGCCTTGC	0.19
*amtB1*_RT R	AAGCCGCCGACGAAGGAATTGAAG	
amtB15		
*amtB15*_RT F	CGCTGTAATGTTGTTAGCCCTG	0.18
*amtB15*_RT R	GCTGGGTGAATACCGAGAGGAAG	
amtB37		
*amtB37*_RT F	GGTGTACTTCTTCATCGGCTACTGGATCG	0.18
*amtB37*_RT R	ACACAGCTGCGGCACAAATCG	
gmaS		
*gmaS*_RT F	TGCTGGCACAGTTCGTCGATATCC	0.17
*gmaS*_RT R	ATCAAGGTAGAAAGGTCGCCGCGG	
mgdC		
*mgdC*_RT F	AGTGCCGAAGCCAAGGTC	0.16
*mgdC*_RT R	GCTTCTCCACGGTCGGCAT	

(Continued on next page)

TABLE 3 (Continued)

Region and primer name	Sequence (5′ to 3′)[a]	Product size (kbp)
mgsC		
*mgsC*_RT F	ATCAAGATTGCCGAGATCCGC	0.17
*mgsC*_RT R	TCGATGAACACTTCCTGAGTCG	
soxA		
*soxA*_RT F	ACCTACGTACGCCGCTACGTGCTTC	0.16
*soxA*_RT R	TTCAACCAGCGAGC	
Primers for cloning of various enzymes		
GMAS		
GMAS_FP	GGAATTCCATATGTTGCCAGCAGAAACC	1.33
GMAS_RP	CCCAAGCTTGAAGAATTCGGTGTAACGCTG	
GS_{C5PP}		
$C5_{PP}GS$_FP	GGAATTCCATATGTCGAAGTCGGTTCAACTC	1.40
$C5_{PP}GS$_RP	CCGGAATTCTCAGCAGCTGTAGTACAGCTCG	
GS_{Ec}		
EcGS_FP	GGAATTCCATATGTCCGCTGAACACGTACTGAC	1.40
EcGS_RP	CCCAAGCTTTTAGACGCTGTAGTACAGCTCAAAC	

[a]Underlined sequences represent the restriction enzyme sites (see Materials and Methods).

each cycle consisted of 15 pulses [11 W] of 1 s each, with an interval of 5 min between two cycles on ice). The cell lysate was centrifuged at 30,000 × *g* for 30 min at 4°C. The clear supernatant obtained was referred to as cell-free extract (CFE) and used for enzyme assays. All enzyme activities were monitored spectrophotometrically (Lambda 35; Perkin Elmer, USA) as described below. Protein estimation was performed by the Bradford method (40) using bovine serum albumin (BSA) as the standard. Specific activities are expressed as nmol·min^{-1}·mg^{-1} of protein.

N-Methylglutamate dehydrogenase (NMGDH) was monitored by measuring the decrease in the absorbance at 600 nm due to the reduction of DCPIP (2,6-dichlorophenol indophenol) (ε_{600} = 18,130 M^{-1}·cm^{-1}) (41). The reaction mixture (1 ml) contained potassium phosphate buffer (67 mM, pH 7.0), DCPIP (57 μM), substrate NMG (670 μM), and an appropriate amount of CFE. The enzymatic rate was calculated after subtracting the observed endogenous reduction of DCPIP in the absence of substrate.

GS and GMAS were monitored by measuring the formation of a reaction product, γ-glutamylhydroxamic acid, at 535 nm (42). The reaction mixture (1 ml) contained imidazole-HCl buffer (50 mM, pH 7.2), $MgCl_2$ (20 mM), β-mercaptoethanol (25 mM), sodium L-glutamate (50 mM), disodium ATP (10 mM), and 50 mM substrate (hydroxylamine hydrochloride for GS or *N*-methylhydroxylamine hydrochloride for GMAS neutralized with 2 N NaOH to pH 7.2). After incubation at 37°C for 20 min, the reaction was terminated by adding 1.5 ml of ferric chloride solution ($FeCl_3$, 0.37 M; HCl, 0.67 N; trichloroacetic acid, 0.2 M). The precipitated proteins were removed by centrifugation at 20,000 × *g* for 15 min, and the absorption of supernatant was read at 535 nm against the reagent blank (consisting of all reaction components except CFE). Under these conditions, an A_{535} of 0.340 corresponds to 1 μmol of γ-glutamylhydroxamic acid (42).

Formaldehyde dehydrogenase (FALDH) was monitored by measuring the increase in absorbance at 340 nm due to the formation of NADH (ε_{340} = 6,220 M^{-1}·cm^{-1}) (43). The reaction mixture (1 ml) contained potassium-phosphate buffer (100 mM, pH 8.0), glutathione (1 mM), NAD^+ (2 mM), formaldehyde (1 mM), and an appropriate amount of CFE.

Glutamate dehydrogenase (GDH) was monitored by measuring the disappearance of NADPH at 340 nm (ε_{340} = 6,220 M^{-1}·cm^{-1}) (44). The reaction mixture (1 ml) contained potassium-phosphate buffer (100 mM, pH 7.5), ammonium chloride (10 mM), α-ketoglutarate (10 mM), NADPH (0.1 mM), and an appropriate amount of CFE. Values from three independent experiments, wherein reactions were performed in triplicate, were used to calculate enzyme activities.

Cloning and overexpression of GMAS and GS. The *gmaS* sequence (1,335 bp) was amplified using genomic DNA of strain C5pp as the template and primers GMAS_FP and GMAS_RP (Table 3). The gel-purified PCR product was digested and cloned at NdeI and HindIII sites into pET-41a(+) (Novagen); this plasmid, named pET41_GMAS, was transformed into *E. coli* BL21(DE3). A single colony obtained was grown on LB plus kanamycin (40 μg·ml^{-1}) at 37°C to an OD_{600} of 0.8. The culture was chilled on ice for 45 min and induced by isopropyl-β-D-thiogalactopyranoside (IPTG) (100 μM) for 16 h at 20°C. Cells were harvested and resuspended (1:10, wt/vol) in potassium-phosphate buffer (50 mM, pH 7.5), and CFE was prepared as described above. CFE prepared from *E. coli* cells carrying vector alone (without the insert) was used as a control.

The *glnA* sequence (1,407 bp) encoding GS was amplified using genomic DNA of strain C5pp as the template and primers C5ppGS_FP and C5ppGS_RP (Table 3). The gel-purified PCR product was digested and cloned at NdeI and EcoRI sites into pET-28a(+) (Novagen). This plasmid, named pET28a(+)_GS_{C5PP}, was transformed into *E. coli* BL21(DE3). A single colony obtained was grown on LB plus kanamycin (40 μg·ml^{-1}) at 37°C to an OD_{600} of 0.8. The culture was chilled on ice for 45 min and induced by IPTG (100 μM) for 6 h at 30°C or 16 h at 20°C. Cells were harvested and resuspended (1:10, wt/vol) in

potassium-phosphate buffer (50 mM, pH 7.5), and CFE was prepared as mentioned above. CFE from *E. coli* cells carrying vector alone (without the insert) was used as a control.

Similarly, the *E. coli* GS open reading frame was amplified (1,410 bp) using its genomic DNA and EcGS_FP and EcGS_RP primers (Table 3). The gel-purified PCR product, digested and cloned at NdeI and EcoRI sites into pET-28a(+) and named pET28a(+)_GS_{Ec}, was overexpressed in *E. coli* under the same conditions as those described for GS_{C5pp}.

Purification of GS_{C5pp} and GS_{Ec}. GS_{C5pp} was purified using Ni-NTA affinity chromatography. Briefly, cells carrying pET28(+)_GS_{C5pp} were induced with IPTG (100 μM, 30°C, 6 h), resuspended in buffer A (50 mM potassium-phosphate buffer, pH 7.5), and disrupted by sonication on ice. The CFE was prepared as described above. The CFE (~60 mg protein) was loaded onto Ni-NTA matrix (80 by 6 mm; bed volume, 10 ml) preequilibrated and washed with buffer A containing imidazole (50 mM, 10 column volumes). Bound GS was eluted using a linear gradient of imidazole in buffer A (50 to 250 mM; flow rate, 30 ml·h^{-1}; fraction size, 2 ml). Active fractions were eluted with 150 to 190 mM imidazole.

GS_{Ec} was purified using the protocol described for GS_{C5pp}, except that the washing buffer was buffer A containing imidazole (20 mM), and the bound enzyme was eluted using a linear gradient of imidazole in buffer A (20 to 250 mM; flow rate, 30 ml·h^{-1}; fraction size, 2 ml). Active fractions were eluted with 170 to 180 mM imidazole.

Active and pure fractions of GS_{C5pp} and GS_{Ec} were analyzed by SDS-PAGE, pooled, dialyzed against buffer A, and used for kinetic characterization. Values from at least two to three independent experiments, wherein reactions were performed in duplicate, were used to calculate kinetic constants.

SUPPLEMENTAL MATERIAL

Supplemental material for this article may be found at https://doi.org/10.1128/AEM.01866-18.

SUPPLEMENTAL FILE 1, PDF file, 1.7 MB.

ACKNOWLEDGMENTS

We thank Rup Lal, Delhi University, for his valuable suggestions and comments. Kamini thanks IIT-B for a teaching assistantship. We acknowledge Vikas Trivedi for preliminary bioinformatic analysis and constructive suggestions and Ferrin Antony and Snehal Bamane for initial help in the optimization of purification conditions. R. Sharma thanks the Director, CSIR-IGIB, for constant support and encouragement.

REFERENCES

1. Latypova E, Yang S, Wang YS, Wang T, Chavkin TA, Hackett M, Schafer H, Kalyuzhnaya MG. 2010. Genetics of the glutamate-mediated methylamine utilization pathway in the facultative methylotrophic beta-proteobacterium *Methyloversatilis universalis* FAM5. Mol Microbiol 75:426–439. https://doi.org/10.1111/j.1365-2958.2009.06989.x.
2. Chen Y, Scanlan J, Song L, Crombie A, Rahman MT, Schafer H, Murrell JC. 2010. γ-Glutamylmethylamide is an essential intermediate in the metabolism of methylamine by *Methylocella silvestris*. Appl Environ Microbiol 76:4530–4537. https://doi.org/10.1128/AEM.00739-10.
3. Anthony C. 1982. Biochemistry of methylotrophs. Academia Press, New York, NY.
4. Neff JM. 2002. Bioaccumulation in marine organisms: effects of contaminants from oil well produced water. Elsevier, Amsterdam, The Netherlands.
5. Bicknell B, Owens JD. 1980. Utilization of methylamines as nitrogen sources by non-methylotrophs. J Gen Microbiol 117:89–96. https://doi.org/10.1099/00221287-117-1-89.
6. Chen Y, McAleer KL, Murrell JC. 2010. Monomethylamine as a nitrogen source for a non-methylotrophic bacterium, *Agrobacterium tumefaciens*. Appl Environ Microbiol 76:4102–4104. https://doi.org/10.1128/AEM.00469-10.
7. Chistoserdova AY, Chistoserdova LV, McIntire WS, Lidstrom ME. 1994. Genetic organization of the *mau* gene cluster in *Methylobacterium extorquens* AM1: complete nucleotide sequence and generation and characteristics of mau mutants. J Bacteriol 176:4052–4065. https://doi.org/10.1128/jb.176.13.4052-4065.1994.
8. Husain M, Davidson VL. 1987. Purification and properties of methylamine dehydrogenase from *Paracoccus denitrificans*. J Bacteriol 169:1712–1717. https://doi.org/10.1128/jb.169.4.1712-1717.1987.
9. Zhang X, Fuller JH, McIntire WS. 1993. Cloning, sequencing, expression, and regulation of the structural gene for the copper/topa quinine-containing methylamine oxidase from *Arthrobacter* strain P1, a Gram-positive facultative methylotroph. J Bacteriol 175:5617–5627. https://doi.org/10.1128/jb.175.17.5617-5627.1993.
10. Gruffaz C, Muller EE, Louhichi-Jelail Y, Nelli YR, Guichard G, Bringel F. 2014. Genes of the *N*-methylglutamate pathway are essential for growth of *Methylobacterium extorquens* DM4 with monomethylamine. Appl Environ Microbiol 80:3541–3550. https://doi.org/10.1128/AEM.04160-13.
11. Wischer D, Kumaresan D, Johnston A, El Khawand M, Stephenson J, Hillebrand-Voiculescu AM, Chen Y, Colin Murrell J. 2015. Bacterial metabolism of methylated amines and identification of novel methylotrophs in Movile Cave. ISME J 9:195–206. https://doi.org/10.1038/ismej.2014.102.
12. Weiden MH. 1971. Toxicity of carbamates to insects. Bull World Health Organ 44:203–213.
13. Sastry KV, Siddiqui AA. 1982. Chronic toxic effects of the carbamate pesticide sevin on carbohydrate metabolism in a freshwater snakehead fish, *Channa punctatus*. Toxicol Lett 14:123–130. https://doi.org/10.1016/0378-4274(82)90019-4.
14. US EPA. 2008. Amended reregistration eligibility decision (RED) for carbaryl. Office of Pesticide Programs, Environmental Protection Agency, Washington, DC.
15. Trivedi VD, Jangir PK, Sharma R, Phale PS. 2016. Draft genome sequence of carbaryl-degrading soil isolate *Pseudomonas* sp. strain C5pp. Genome Announc 4:e00526-16. https://doi.org/10.1128/genomeA.00526-16.
16. Chapalamadugu S, Chaudhry GR. 1991. Hydrolysis of carbaryl by a *Pseudomonas* sp. and construction of a microbial consortium that completely metabolizes carbaryl. Appl Environ Microbiol 57:744–750.
17. Mulbry WW, Eaton RW. 1991. Purification and characterization of the *N*-methylcarbamate hydrolase from *Pseudomonas* strain CRL-OK. Appl Environ Microbiol 57:3679–3682.
18. Hayatsu M, Mizutani A, Hashimoto M, Sato K, Hayano K. 2001. Purification and characterization of carbaryl hydrolase from *Arthrobacter* sp. RC100. FEMS Microbiol Lett 201:99–103. https://doi.org/10.1111/j.1574-6968.2001.tb10739.x.

19. Swetha VP, Phale PS. 2005. Metabolism of carbaryl via 1,2-dihydroxynaphthalene by soil isolates *Pseudomonas* sp. strains C4, C5, and C6. Appl Environ Microbiol 71:5951–5956. https://doi.org/10.1128/AEM.71.10.5951-5956.2005.
20. Seo JS, Keum YS, Li QX. 2013. Metabolomic and proteomic insights into carbaryl catabolism by *Burkholderia* sp. C3 and degradation of ten *N*-methylcarbamates. Biodegradation 24:795–811. https://doi.org/10.1007/s10532-013-9629-2.
21. Hamada M, Matar M, Bashir A. 2015. Carbaryl degradation by bacterial isolates from a soil ecosystem of the Gaza Strip. Braz J Microbiol 46:1087–1091. https://doi.org/10.1590/S1517-838246420150177.
22. Kamini, Shetty D, Trivedi VD, Varunjikar M, Phale PS. 2018. Compartmentalization of carbaryl degradation pathway: molecular characterization of inducible periplasmic carbaryl hydrolase from *Pseudomonas* spp. Appl Environ Microbiol 84:02115-17. https://doi.org/10.1128/AEM.02115-17.
23. Taguchi K, Kudo T, Tobari J. 1997. Genetic organization and characterization of the mau gene cluster, which concerned the initial step of electron transport chains involved in methylamine oxidation of the obligate methylotroph *Methylomonas* sp. strain J. J Ferment Bioeng 84:502–510. https://doi.org/10.1016/S0922-338X(97)81902-2.
24. Liaw SH, Kuo I, Eisenberg D. 1995. Discovery of the ammonia substrate site on glutamine synthetase, a third cation binding site. Protein Sci 4:2358–2365. https://doi.org/10.1002/pro.5560041114.
25. Yamamoto S, Wakayama M, Tachiki T. 2008. Cloning and expression of *Methylovorus mays* no. 9 gene encoding gamma-glutamylmethylamide synthetase: an enzyme usable in theanine formation by coupling with the alcoholic fermentation system of baker's yeast. Biosci Biotechnol Biochem 72:101–109. https://doi.org/10.1271/bbb.70462.
26. Udvardi MK, Day DA. 1990. Ammonia (^{14}C-methylamine) transport across the bacteriod and peribacteriod membranes of soybean root nodules. Plant Physiol 94:71–76. https://doi.org/10.1104/pp.94.1.71.
27. Marini AM, Soussi-Boudekou S, Vissers S, Andre B. 1997. A family of ammonium transporters in *Saccharomyces cerevisiae*. Mol Cell Biol 17:4282–4293. https://doi.org/10.1128/MCB.17.8.4282.
28. He S, Chen M, Xie Z, Yan Y, Li H, Fan Y, Ping S, Lin M, Elmerich C. 2008. Involvement of GlnK, a pll protein, in control of nitrogen fixation and ammonia assimilation in *Pseudomonas stutzeri* A1501. Arch Microbiol 190:1–10. https://doi.org/10.1007/s00203-008-0354-x.
29. Suzuki H, Tamamura R, Yajima S, Kanno M, Suguro M. 2005. *Corynebacterium* sp. U-96 contains a cluster of genes of enzymes for the catabolism of sarcosine to pyruvate. Biosci Biotechnol Biochem 69:952–956. https://doi.org/10.1271/bbb.69.952.
30. Chen Z, W Hassan-Abdulah A, Zhao G, Jorns MS, Mathews FS. 2006. Heterotetrameric sarcosine oxidase: structure of a diflavin metalloenzyme at 1.85 Å resolution. J Mol Biol 360:1000–1018. https://doi.org/10.1016/j.jmb.2006.05.067.
31. Chlumsky LJ, Zhang L, Jorns MS. 1995. Sequence analysis of sarcosine oxidase and nearby genes reveals homologies with key enzymes of folate one-carbon metabolism. J Biol Chem 270:18252–18259. https://doi.org/10.1074/jbc.270.31.18252.
32. Bellion E, Kent ME, Aud JC, Alikhan MY, Bolbot JA. 1983. Uptake of methylamine and methanol by *Pseudomonas* sp. strain AM1. J Bacteriol 154:1168–1173.
33. Barnes EM, Jr, Zimniak P, Jayakumar A. 1983. Role of glutamine synthetase in the uptake and metabolism of methylammonium by *Azotobacter vinelandii*. J Bacteriol 156:752–757.
34. Levitch ME. 1976. The demonstration of two discrete enzymes catalyzing the synthesis of glutamine and gamma-glutamylmethylamide in *Pseudomonas* MS. Biochem Biophys Res Commun 76:609–614.
35. Altschul SF, Gish W, Miller W, Myers EW, Lipman DJ. 1990. Basic local alignment search tool. J Mol Biol 215:403–410. https://doi.org/10.1016/S0022-2836(05)80360-2.
36. Tamura K, Stecher G, Peterson D, Filipski A, Kumar S. 2013. MEGA6: Molecular Evolutionary Genetics Analysis version 6.0. Mol Biol Evol 30:2725–2729. https://doi.org/10.1093/molbev/mst197.
37. Omasits U, Ahrens CH, Muller S, Wollscheid B. 2014. Protter: interactive protein feature visualization and integration with experimental proteomic data. Bioinformatics 30:884–886. https://doi.org/10.1093/bioinformatics/btt607.
38. Bertani G. 1951. Studies on lysogenesis. I. The mode of phage liberation by lysogenic *Escherichia coli*. J Bacteriol 62:293–300.
39. Livak KJ, Schmittgen TD. 2001. Analysis of relative gene expression data using real-time quantitative PCR and $2^{-\Delta\Delta}CT$ method. Methods 25:402–408. https://doi.org/10.1006/meth.2001.1262.
40. Bradford MM. 1976. A rapid and sensitive method for the quantitation of microgram quantities of protein utilizing the principle of protein-dye binding. Anal Biochem 72:248–254. https://doi.org/10.1016/0003-2697(76)90527-3.
41. Bamforth CW, Large PJ. 1977. Solubilization, partial purification and properties of *N*-methylglutamate dehydrogenase from *Pseudomonas aminovorans*. Biochem J 161:357–370. https://doi.org/10.1042/bj1610357.
42. Rowe B. 1970. Glutamine synthetase (sheep brain). Methods Enzymol 17:900–910. https://doi.org/10.1016/0076-6879(71)17304-1.
43. Kato N. 1990. Formaldehyde dehydrogenase from methylotrophic yeasts. Methods Enzymol 188:455–459. https://doi.org/10.1016/0076-6879(90)88072-I.
44. Vamsee-Krishna C, Phale PS. 2008. Carbon source-dependent modulation of NADP$^-$ glutamate dehydrogenases in isophthalate-degrading *Pseudomonas aeruginosa* strain PP4, *Pseudomonas* strain PPD and *Acinetobacter lwoffii* strain ISP4. Microbiology 154:3329–3337. https://doi.org/10.1099/mic.0.2008/022087-0.